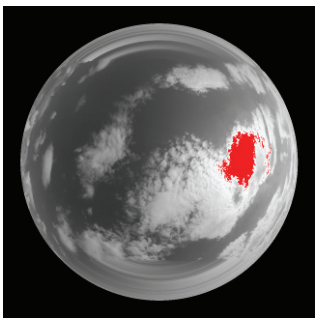

Fig. 1. Saturated pixels in the sky hemisphere picture

The ratio then used in calculation of radiance centre of hemisphere by adjusting saturated pixels relative luminances

$$L_{x,y} = \frac{\sum_{x=1}^{x_{max}} \sum_{y=1}^{y_{max}} L'_{x,y} \cdot \frac{\left(I_{full} - I_{scattered}\right)}{\cos\varphi}}{n_{saturated} \cdot k \cdot I_{scattered}}, \quad (3)$$

where $L_{x,y}$ – relative luminance of saturated pixel at coordinates x and y; $L'x,y$ – relative luminance of a non saturated pixel at coordinates x and y; I_{full} – measured irradiance of full hemisphere; $I_{scattered}$ – measured irradiance of hemisphere with shadowed sun; $n_{saturated}$ – number of saturated pixels; φ – sun/saturated blob incandescence angle, k – correction coefficient.

Provided formula assumes that luminance distribution is uniform within saturated pixels. That is a reasonable approximation for the task.

Purpose of coefficient k is to compensate difference in the shape of radiance/luminance capturing body. Pyranometer has flat sensing element with maximum sensitivity at the zenith and zero sensitivity at the horizon. Fish eye lens is of a hemisphere shape. Sky dome radiance distribution mathematical model was created to evaluate the difference.

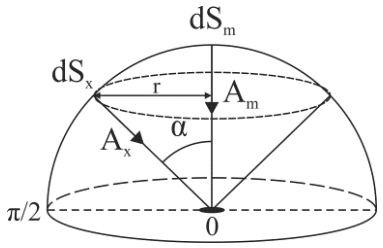

Fig. 2. Radiance vectors in the sky dome

The sum of all radiance vectors A_{sum} is described by using cone surface area formula (Fig. 2)

$$A_{sum} = \int_0^{\frac{\pi}{2}} \pi \cdot A_x(\alpha) \cdot \sin(\alpha) \cdot A_x(\alpha) \cdot d\alpha, \quad (4)$$

where A_x – radiance at α incidence, A_m – radiance at zenith. For pyranometer like reception A_x will be

$$A_x(\alpha) = A_m \cdot \cos(\alpha). \quad (5)$$

For fish eye lens like reception A_x will be:

$$A_x(\alpha) = A_m. \quad (6)$$

Therefore sum radiances A_{sum_p} and A_{sum_i} for each case will be:

$$A_{sum\_p} = \int_0^{\frac{\pi}{2}} \pi \cdot A_m^2 \cdot \cos^2(\alpha) \cdot \sin(\alpha) \cdot d\alpha, \quad (7)$$

$$A_{sum\_i} = \int_0^{\frac{\pi}{2}} \pi \cdot A_m^2 \cdot \sin(\alpha) \cdot d\alpha. \quad (8)$$

Correction coefficient for formula (3) calculated

$$k = \frac{A_{sum\_i}}{A_{sum\_p}}. \quad (9)$$

For 180° hemisphere shape of fish eye lens k equals 3. During the experimental work there was made a 10° cut just above the horizon to avoid obstacles like trees and houses and it reduces the k to 2.74. It must be noted that there is an approximation made when calculating correction coefficient with this model that sky dome radiance is uniform. This considered a reasonable approximation for the task.

Relative luminance of a pixel in the photo picture is calculated from R, G, B values extracted from corresponding pixel in the picture

$$L_{xy} = 0.2125 \cdot R_{xy} + 0.7154 \cdot G_{xy} + 0.0721 \cdot B_{xy}. \quad (10)$$

Experimental

Series of experiments have been accomplished to put algorithm under test. It was attempted to estimate thermal radiance center in the sky by new algorithm, by industry standard solar sensor and by measuring radiance distribution itself. A test rig was built for the experiment. It consisted of:

- DSLR camera equipped with fish-eye lens;
- Pyranometer without shadow, to measure full irradiance;
- Pyranometer with shadow, to measure scattered irradiance;
- GPS receiver for having precise time;
- A positioning system with spectrum analyzer;
- PC with dedicated software for control tasks and data storage, built using typical design patterns[4].

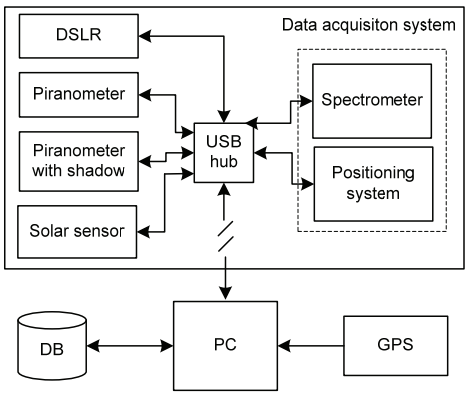

Fig. 3. Measurement rig block diagram

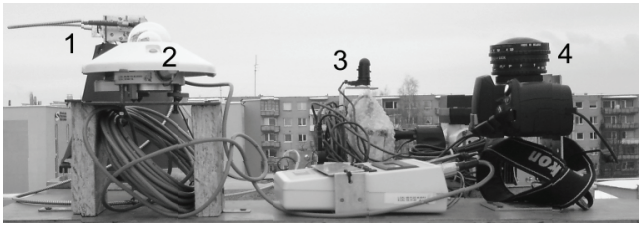

Fig. 4. Measurement system situated on the roof (1 – relative radiance scanner with spectrometer, 2 – pyranometer without shadow, 3 – automotive solar sensor, 4 – DSLR camera

A system was built to be reliable in long continuous measurement test sessions [5].

A separate investigation has been done to find out how uniformly fish-eye lens transfers the light to DSLR sensor. Investigation showed that relative luminance difference of the same source of luminance between the centre of picture and at 170º off centre is 25% and it does change linearly. Appropriate compensation for each individual pixel was made during picture processing.

There was taken 170º hemisphere for evaluation instead of 180º, since the area just above the horizon was filled with surrounding city obstacles.

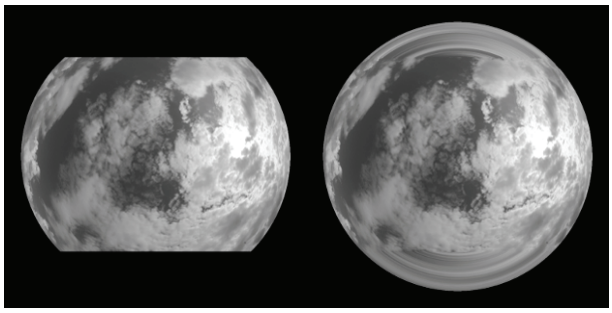

Fig. 5. Interpolation of missing pixels

The fish eye lens that was used (MS Peleng 3.5/8A) does not allow capturing full hemisphere picture. It does cut it in two directions. Hence interpolation technique was used to extract the missing data from present picture pattern (Fig. 3). A linear transition formula was applied

$$L_{\alpha,\beta} = \frac{\Delta L_\beta}{\Delta \alpha_\beta} \cdot \alpha \,, \qquad (11)$$

where $L_{\alpha,\beta}$ is a pixel relative luminance at angles azimuth α and elevation β; ΔL_β is a change in relative luminance in each end of a missing circular line at elevation β, $\Delta\alpha_\beta$ is an azimuth change angle of a missing circular line at elevation β.

For radiance distribution measurement a USB4000 fiber optic spectrometer was used. It has spectrum measurements bandwidth of 200 to 1100 nm. Optical collimator at the end of the fiber wire had an acceptance angle of 2,7°. The hemisphere has been scanned at 145 equally spread zones, by employing specially built, PC controlled, positioning rig. Combining all 145 zones into 2D projection, corresponding to hemisphere picture, a sky hemisphere map of relative radiance has been acquired. It then was overlaid on hemisphere picture for comparison. Spectrum integration time had been adjusted dynamically by the software in order to have peak of a spectrum higher than 2/3'ds of maximum measureable value of 16 bit ADC to preserve signal resolution. Relative radiance energy was estimated by the following formula out of spectrum reading (Fig. 6)

$$E_Z = \frac{\sum_{\lambda=200}^{1100} A_\lambda}{t_i} \,, \qquad (12)$$

where E_Z – relative zone Z radiance energy, A_λ – spectrum amplitude at wavelength λ, t_i – spectrum measurement integration time.

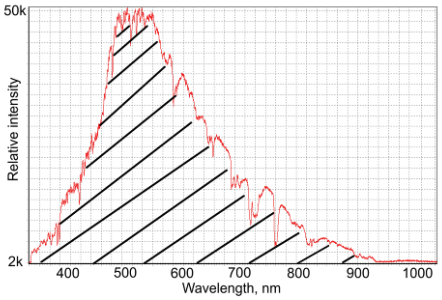

Fig. 6. Sample of measured spectrum

Since integration varies dynamically depending on radiation intensity, so does the total time of scan. At clear sky conditions having 800W/m2 global irradiation, scanning took around 60 seconds. At lower irradiation levels scanning time stretched. Hence weather conditions were picked having low wind velocity to have cloud composition as static as possible for the scan duration. GPS reading, picture of hemisphere and solar sensor reading are taken within a second after measurement cycle start. The system was put on the roof of four floor building to have as much obstacle-clear sky as possible. All instruments where mounted on a platform which was aligned to horizon plane. Solar sensor, positioning system and DSLR camera were aligned to each other, so that it would be possible to combine measurements of different devices together.

An example of relative radiance distribution estimated with the test rig showed in Fig. 5.

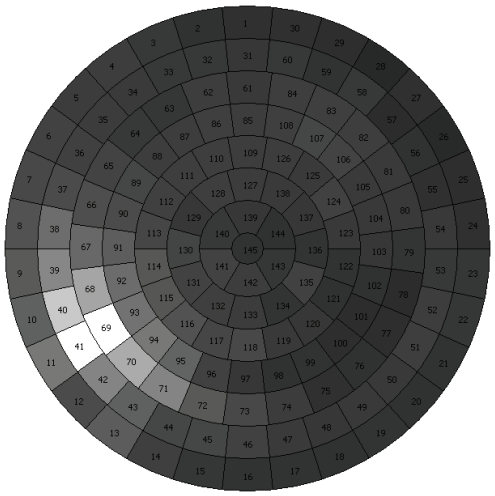

Fig. 7. An example of relative radiance scans

During the measurement or relative radiance with spectrometer the problem of lack of dynamic range was experienced in the zones with sun present. It was solved the same way like with photo picture saturated pixels. The same algorithm implementation was used by turning Fig. 7 visual relative radiance representation into Fig. 1 like picture. Formula (3) was used to compensate saturated areas with by pyranometers acquired ratio between the saturated area and the non-saturated area irradiances.

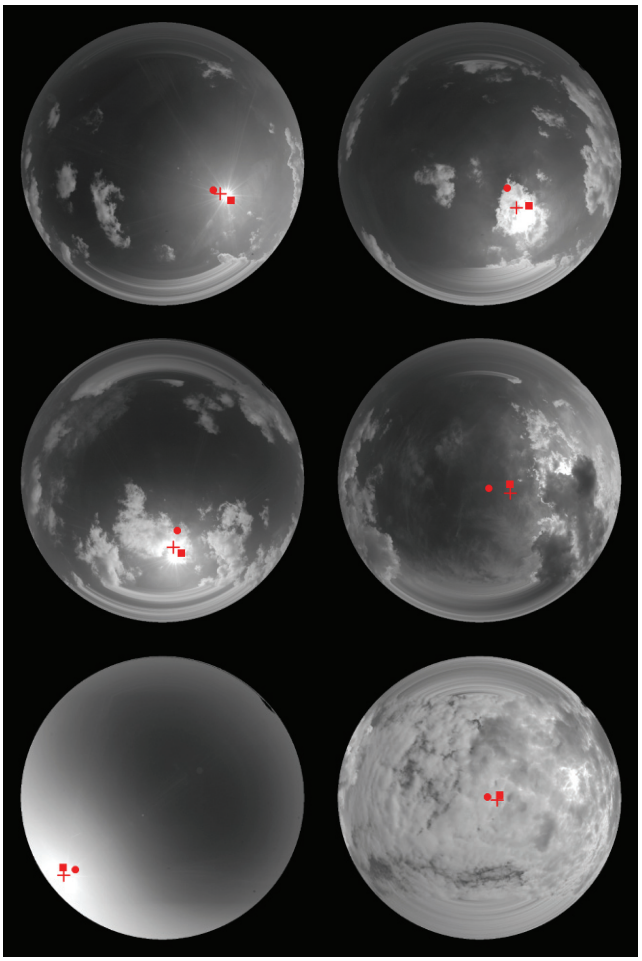

Fig. 8. Samples of sky hemispheres and estimated thermal radiance centers

Numerous test sessions were made with different cloud compositions and sun positions in the sky hemisphere. Samples of typical hemispheres are shown in figure 8 with marks pointing to a location of thermal radiance centers estimated with proposed algorithm. Cross mark points to calculated position by using DSLR camera picture, square mark points to position calculated using radiance distribution scanner and round mark points to solar sensors measured position.

Conclusions

An algorithm was proposed how to estimate thermal radiance center in the sky hemisphere as an angular position of azimuth and elevation. Estimation of this position is relevant for producers of automotive solar sensors, who face the absence of standard on what is the position of radiance source in the sky hemisphere. Furthermore, current commercial sky hemisphere radiance distribution readers are too expensive for using them in industry validation processes. The proposed algorithm provides significant simplification and reduction in cost, therefore potentially could be used in industry validation process.

References

1. **Jačėnas S., Gailius D.** Thermal comfort, sky dome radiant heat and solar sensors in vehicles // Matavimai. – Kaunas: Technologija, 2009. – Nr. 1(43). – P. 23–26.
2. **Vasarevičius D., Martavičius R.** Solar Irradiance Model for Solar Electric Panels and Solar Thermal Collectors in Lithuania // Electronics and Electrical Engineering. – Kaunas: Technologija, 2011. – No. 2(108). – P. 3–6.
3. **Norio Igawa, Yasuko Koga, Tomoko Matsuzawa, Hiroshi Nakamura.** Models of sky radiance distribution and sky luminance distribution // Solar Energy, 2004. – Vol. 77. – Iss. 2. – P. 137–157.
4. **Ezerskis D., Simutis R.** Valdymo uždavinių programavimas taikant projektavimo šablonų rinkinį // Elektronika ir elektrontechnika. – Kaunas: Technologija, 2005. – Nr. 5(61). – P. 94–99.
5. **Balaišis R. J., Balaišis P., Eidukas D.** Elektroninių valdymo įtaisų patikimumo aspektai // Elektronika ir elektrotechnika. – Kaunas: Technologija, 1998. – Nr. 4(17). – P. 58–62.

Received 2011 05 03

S. Jacenas. An Algorithm to Estimate Thermal Radiance Centre in the Sky Hemisphere for Automotive Solar Sensor Validation // Electronics and Electrical Engineering. – Kaunas: Technologija, 2011. – No. 6(112). – P. 73–76.

There is a solar sensor used in vehicles to estimate thermal radiance source position (azimuth and elevation) in the sky hemisphere and the amplitude of irradiance. That data is used for adjusting climate control systems for maximum passengers comfort in vehicle cabin. Producers of such sensors face the absence of standard on what is the position of radiance source in the sky hemisphere. Furthermore, current means to measure radiance distribution are very expensive. An algorithm was proposed to estimate thermal radiance center position, by means of standard DSLR camera equipped with fish-eye lens. The algorithm was put under test by implementing series of experiments. Result samples of the thermal radiance center estimated by sensor and by proposed algorithm where presented. Ill. 8, bibl. 5 (in English; abstracts in English and Lithuanian).

S. Jačėnas. Dangaus skliauto šiluminės spinduliuotės centro nustatymo algoritmas, pritaikomas automobilinių saulės jutiklių kokybės analizei // Elektronika ir elektrotechnika. – Kaunas: Technologija, 2011. – Nr. 6(112). – P. 73–76.

Automobilių pramonėje naudojami saulės jutikliai vertina šiluminės spinduliuotės šaltinio kryptį automobilio atžvilgiu ir intensyvumą. Duomenys naudojami klimato kontrolės sistemoje šiluminiams oro srautams reguliuoti taip kuriant ištaigų mikroklimatą automobilio salone. Tačiau tokių jutiklių gamintojai susiduria su problema – automobilių pramonėje nėra aiškiai apibrėžta, kas tai yra šiluminės spinduliuotės centras dangaus skliaute. Be to, dabartiniai šiluminio pasiskirstymo dangaus skliaute matavimo prietaisai yra labai brangūs, todėl jutiklių gamintojai jų nenaudoja. Buvo pasiūlytas algoritmas, kaip įvertinti šiluminės spinduliuotės centrą naudojant standartinį DSLR fotoaparatą su žuvies akies lęšiu. Atlikta serija šio algoritmo bandymų. Pateikta rezultatų pavyzdžių. Il. 8, bibl. 5 (anglų kalba; santraukos anglų ir lietuvių k.).